Neutrino Portal to Freeze-in Dark Matter

P. S. Bhupal Dev

Department of Physics and McDonnell Center for the Space Sciences, Washington University, St. Louis, MO 63130, USA

Abstract

We investigate the possibility of probing freeze-in dark matter (DM) produced via the heavy neutral lepton (HNL) portal at the HNL frontier within the framework of the type-I seesaw. We consider two cases for the DM production either via decay of the thermal HNL or via scattering of the bath particles mediated by the HNL. In both cases, we show that the allowed model parameter space satisfying the observed DM relic density for the freeze-in scenario remains within reach of several HNL search experiments.

Keywords: neutrino, dark matter, HNL frontier
DOI: 10.31526/LHEP.2022.356

1. INTRODUCTION

The nature of dark matter (DM) remains enigmatic. The DM couplings to the Standard Model (SM) sector are not known, except for their gravitational effects. Any nongravitational DM interactions with the SM would require some beyond the SM (BSM) physics.

Among various possible particle DM candidates [1], the Weakly Interacting Massive Particle (WIMP) [2] paradigm initially gained a lot of traction, because of its miraculous property of being able to reproduce the observed relic abundance via weak-scale interaction cross sections for a wide range of DM masses [3]. The basic idea is that at high temperatures, the DM particles are in thermal equilibrium but as the temperature falls below roughly one-twentieth of the DM mass, equilibrium is lost and the DM particles *freeze out* of the thermal plasma. However, in spite of being so appealing, the WIMP scenario has been waning lately, due to stringent experimental tests from direct detection, indirect detection, and collider searches [4, 5]. This has motivated quests for DM beyond the WIMP paradigm [6].

Since DM is electrically neutral, a simple alternative to the WIMP paradigm is to have the DM as a pure singlet under the SM gauge group. In this case, the DM can interact with the SM sector only via the so-called "portals." There exist only three such portals in the SM, depending on whether the mediator has spin-0 (Higgs portal) [7, 8], spin-1 (vector portal) [9, 10], or spin-1/2 (neutrino portal) [11, 12]. In this talk, we will focus on the neutrino portal scenario which is particularly interesting because of its intimate connection to neutrino mass—another outstanding puzzle that also calls for some BSM physics. For related discussion, see [11, 12, 13, 14, 15, 16, 17, 18, 19, 20, 21, 22, 23, 24, 25, 26, 27, 28, 29, 30, 31, 32, 33, 34, 35, 36, 37, 38, 39, 40].

A simple realization of the neutrino portal relies on DM interactions being mediated by SM gauge-singlet fermions, also known as heavy neutral leptons (HNLs). The HNLs are well motivated by the type-I seesaw mechanism for neutrino mass generation [41, 42, 43, 44, 45, 46]. Depending on their mass and Dirac Yukawa couplings, which together determine their mixing with the SM neutrinos, the HNLs can be searched for in a wide range of experiments, such as beta decay, meson decay, beam dump, and colliders; for a comprehensive summary of the existing constraints and future prospects of HNL searches; see, e.g., [47, 48]. In this talk, based on our recent work [40], we show that the same HNL parameter space that can be probed in future experiments can also reproduce the observed DM relic density via the *freeze-in* mechanism [49].

In our case, the HNLs are the only mediators between the SM and the DM sectors. In addition, the portal couplings to the dark sector are sufficiently small so that the DM never reaches chemical equilibrium with the thermal bath. The DM is slowly populated in the Universe by either decay or annihilation processes involving the HNLs, until the production ceases due to Boltzmann suppression as the Hubble temperature drops below the HNL mass. Due to their tiny interaction strength with the visible sector, freeze-ins are inherently very difficult to search for directly in conventional DM direct detection, indirect detection, or collider experiments [50]. However, unlike freeze-out, for freeze-in, one typically looks for signatures of the portal itself and its associated tiny couplings. For instance, the feeble couplings associated with the portal could make either the heavier dark sector particles or the mediator itself long-lived, leading to signatures in lifetime and intensity frontier experiments [51]. Other examples involving properties of the individual BSM models like kinetic mixing [52], temperature corrections [53], and scale-invariance [54, 55] have been proposed for the freeze-in mechanism that can be searched for in direct detection experiments as well. Similarly, a nonstandard cosmological era can also make freeze-in sensitive to indirect detection [32]. As we demonstrate in this talk, the HNL portal effectively provides a complementary laboratory probe of the freeze-in DM scenario.

2. THE MODEL

We add to the SM particle content the following:

(i) SM gauge-singlet HNLs N_i. We need at least two HNLs (i.e., $i = 1, 2$) in order to reproduce two nonzero mass-squared differences, as observed in neutrino oscillation data, using the seesaw mechanism. For our current interest, a hierarchical spectrum can be assumed, so that only the lightest HNL N_1 will be relevant for us.

(ii) A gauge-singlet Majorana fermion χ which serves as the DM candidate. Note that a Dirac fermion would also serve the purpose, but at the expense of doubling the degrees of freedom.

(iii) A real singlet scalar φ which is needed to connect the DM to the HNL portal.

We will assume that both χ and φ are charged under a Z_2 symmetry and that χ is lighter than φ to ensure the stability of the

DM. The SM particles and the HNLs are assumed to be even under this Z_2 symmetry, which forbids couplings between SM and dark sector particles (χ, φ). The relevant piece of the Lagrangian giving rise to neutrino mass is given by

$$-\mathcal{L}_\nu = (Y_D)_{\alpha j}\,\overline{L}_\alpha H N_j + \frac{1}{2}\,(M_N)_{ij}\,\overline{N_i^c} N_j + \text{H.c.}, \tag{1}$$

where L and H are the $SU(2)_L$ lepton and Higgs doublets respectively, and $\alpha = e, \mu, \tau$ is the flavor index. The interaction Lagrangian for the dark sector containing the singlet Majorana DM χ and the real singlet scalar φ reads

$$-\mathcal{L}_{\text{dark}} = y_\chi \overline{N^c}\varphi\chi + m_\chi \overline{\chi^c}\chi + V(H,\varphi) + \text{H.c.}, \tag{2}$$

where $V(H,\varphi)$ is the scalar potential (see below), and we have assumed a universal coupling of DM to the HNLs. The HNLs serve as the portal to mediate the interactions between the dark and visible sectors, owing to the couplings Y_D and y_χ. Note that the same Y_D is also involved in active-sterile neutrino mixing, leading to light neutrino mass generation via type-I seesaw mechanism.

Once the SM Higgs doublet gets a nonzero vacuum expectation value (VEV)

$$H = \frac{1}{\sqrt{2}}\begin{pmatrix} 0 \\ h+v \end{pmatrix} \tag{3}$$

with $v \simeq 246\,\text{GeV}$, we obtain the Dirac mass matrix $M_D = Y_D\langle H\rangle$. The singlet scalar φ, on the other hand, does not acquire a VEV, and therefore, there is no mixing between the DM and the HNLs. The Lagrangian in equation (1) in the flavor basis then reads

$$-\mathcal{L}_\nu = \frac{1}{2}\begin{pmatrix}\overline{(\nu_L)^c} & \overline{N}\end{pmatrix}\mathcal{M}\begin{pmatrix}\nu_L \\ N^c\end{pmatrix} + \text{H.c.}, \tag{4}$$

where the mass matrix can be realized as

$$\mathcal{M} = \begin{pmatrix} 0 & M_D \\ M_D^T & M_N \end{pmatrix}, \tag{5}$$

which can be diagonalized using a unitary matrix $\mathcal{U}$:

$$\mathcal{M}_{\text{diag}} = \mathcal{U}^T \cdot \mathcal{M} \cdot \mathcal{U}, \tag{6}$$

obtaining masses of the neutrinos on a physical basis. We work in a basis where M_N is diagonal, i.e., $\widehat{M}_N \equiv M_N = \text{diag}(M_1, M_2)$, and express the Yukawa matrix following the Casas-Ibarra (CI) parametrization [56] as

$$Y_D = \frac{\sqrt{2}}{v}\sqrt{\widehat{M}_N}\,\mathbb{R}\sqrt{\widehat{m}_\nu}\,U_{\text{PMNS}}^\dagger, \tag{7}$$

with U_{PMNS} being the PMNS matrix that diagonalizes the active neutrino sector (ignoring any nonunitarity effects) $\widehat{m}_\nu = \text{diag}(m_1, m_2, m_3)$, while $\mathbb{R}$ is an arbitrary complex orthogonal rotation matrix with $\mathbb{R}^T\mathbb{R} = \mathbb{I}$. In the minimal seesaw scenario with two HNLs [57], considering normal hierarchy (NH) among the light neutrino masses, one can define the rotation matrix as

$$\mathbb{R}_{\text{NH}} = \begin{pmatrix} 0 & \cos z & \sin z \\ 0 & -\sin z & \cos z \end{pmatrix}, \tag{8}$$

where z is in general a complex angle. This choice automatically implies that the lightest active neutrino is massless. The mass eigenstates can be defined via the unitary rotation:

$$\begin{pmatrix}\nu_L \\ N^c\end{pmatrix} = \mathcal{U}\begin{pmatrix}\nu_i \\ N_j\end{pmatrix}, \tag{9}$$

and the matrix $\mathcal{U}$ can be expressed as (expanding in terms of $M_D M_N^{-1}$)

$$\mathcal{U} = \begin{pmatrix} U_{\nu\nu} & U_{\nu N} \\ U_{N\nu} & U_{NN} \end{pmatrix}. \tag{10}$$

In terms of the CI parametrization (cf. equation (7)), to leading order, we find [58, 32]

$$\begin{aligned} U_{\nu\nu} &\approx U_{\text{PMNS}}, \\ U_{\nu N} &\approx M_D^\dagger M_N^{-1} = \sqrt{2}U_{\text{PMNS}}\sqrt{\widehat{m}_\nu}\,\mathbb{R}^\dagger M_N^{-1/2}, \\ U_{N\nu} &\approx -M_N^{-1} M_D U_{\nu\nu} = -\sqrt{2}M_N^{-1/2}\mathbb{R}\sqrt{\widehat{m}_\nu}, \\ U_{NN} &\approx \mathbb{I}. \end{aligned} \tag{11}$$

The charged current interaction vertices are then modified as

$$\mathcal{L}_{\text{CC}} \supset \frac{g}{\sqrt{2}}\left[(U_{\nu\nu})_{\alpha i}\,\overline{\ell}_{L\alpha}\gamma^\mu \nu_i + (U_{\nu N})_{\alpha j}\,\overline{\ell}_{L\alpha}\gamma^\mu N_j + \text{H.c.}\right] W_\mu^- \tag{12}$$

(g being the $SU(2)_L$ gauge coupling strength), whereas the neutral current interaction vertices are modified as

$$\begin{aligned} \mathcal{L}_{\text{NC}} \supset \frac{g}{2\cos\theta_w} \Big[&\left(U_{\nu\nu}^\dagger U_{\nu\nu}\right)_{ij} \overline{\nu}_i\gamma^\mu\nu_j \\ &+ \left(U_{\nu N}^\dagger U_{\nu N}\right)_{kl} \overline{N}_k\gamma^\mu N_l \\ &+ \left(U_{\nu N}^\dagger U_{\nu\nu}\right)_{ki} \overline{N}_k\gamma^\mu\nu_i \\ &+ \left(U_{\nu\nu}^\dagger U_{\nu N}\right)_{ik} \overline{\nu}_i\gamma^\mu N_k \Big] Z_\mu, \end{aligned} \tag{13}$$

where θ_w is the weak mixing angle, and we have utilized $U_{\nu N}^T M_D = \widehat{m}_\nu U_{\nu\nu}^\dagger$ and $U_{NN}^T M_D = M_N U_{\nu N}^\dagger$. Similarly, the DM-neutrino interaction Lagrangian can be written in the physical basis as

$$-\mathcal{L}'_{\text{dark}} \supset y_\chi \sum_k \left[\left(U_{N\nu}^T\right)_{ki}\overline{\nu}_i\varphi\chi + \left(U_{NN}^T\right)_{kj}\overline{N}_j\varphi\chi\right] + \text{H.c.} \tag{14}$$

The renormalizable scalar potential (cf. equation (2)) involving the two scalars of the theory, namely, $\{\varphi, H\}$ is given by

$$\begin{aligned} V(H,\varphi) = &-\mu_H^2\left(H^\dagger H\right) + \lambda_H\left(H^\dagger H\right)^2 \\ &+ \mu_\varphi^2\varphi^2 + \lambda_\varphi\varphi^4 + \lambda_{H\varphi}\varphi^2\left(H^\dagger H\right). \end{aligned} \tag{15}$$

After electroweak symmetry breaking, the scalar mass matrix is given by

$$\mathbb{M}^2 = \begin{pmatrix} 2v^2\lambda_H & 0 \\ 0 & \lambda_{H\varphi}v^2 + 2\mu_\varphi^2 \end{pmatrix}, \tag{16}$$

where the two terms can be identified as the squared masses of the SM Higgs h and the singlet φ, respectively.

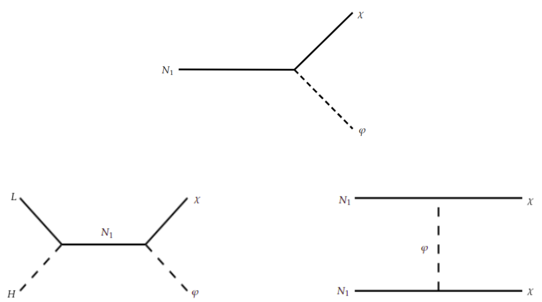

FIGURE 1: Relevant dark matter production channels via 1-to-2 decay (top) 2-to-2 scattering (bottom) involving the HNLs.

3. FREEZE-IN DARK MATTER

In the present set-up, the DM can be produced via (a) on-shell decay of HNL if $M_N > m_\chi + m_\varphi$, or (b) 2-to-2 scatterings mediated by HNL. In case a decay is present, the scattering will be subdominant; hence, in the following, we treat DM production from decay and that from scattering separately. We assume that the lightest HNL N_1 is responsible for freeze-in production of DM. Now, since freeze-in happens when thermal bath species produce DM via out-of-equilibrium processes, it is important to know whether the HNLs thermalize with the SM particles during the freeze-in production. As argued in [59, 60], in low-scale type-I seesaw models with three extra sterile states, full thermalization in the early Universe is always reached for three HNL states if the lightest neutrino mass is above $\mathcal{O}(10^{-3})$ eV, while if the lightest neutrino mass is below $\mathcal{O}(10^{-3})$ eV, only one of the sterile states might never thermalize. Thus, in the subsequent analysis, we will consider the freeze-in production to be happening from the thermal bath containing the HNLs.

The relevant DM production channels are shown in Figure 1:

(i) Decay: $N_1 \to \chi\varphi$ (top panel)

(ii) s-channel HNL mediated scattering: $LH \to \chi\varphi, VL \to \chi\varphi$ with $V \in W^\pm, Z$ (bottom left).

(iii) t-channel φ mediated scattering: $N_1 N_1 \to \chi\chi$ (bottom right).

The Boltzmann equation (BE) governing the DM number density can be written in terms of the DM yield defined as a ratio of the DM number density to the entropy density in the visible sector, i.e., $Y_\chi = n_\chi/s$. The BE can then be expressed in terms of the reaction densities as

$$x H s \frac{dY_\chi}{dx} = \gamma_{\rm ann} + \gamma_{\rm decay}, \tag{17}$$

where $x \equiv m_\chi/T$ is a dimensionless quantity. The complete expressions for the reaction densities γ_i's can be found in [40]. Since we investigate a feebly coupled sector, the back reactions in the DM production processes can be neglected [49].

3.1. Comparison of the Rates

It is important to ensure that the DM does not thermalize with the SM bath in the early Universe, which is the primary requirement for freeze-in. Assuming that the $N \to \varphi\chi$ decay is kinematically available, we first find the region compatible with freeze-in from the requirement of $\langle\Gamma_{N\to\varphi\chi}\rangle < \mathcal{H}$, where we have defined the thermally averaged decay width of HNL into DM as

$$\langle\Gamma_{N\to\varphi\chi}\rangle = \Gamma_{N\to\varphi\chi}\frac{K_1(M_1/T)}{K_2(M_1/T)}, \tag{18}$$

where $\Gamma_{N\to\varphi\chi} \simeq y_\chi^2 M_1/(8\pi)$; $M_1 \gg m_{\varphi,\chi}$ is the decay width of N_1 into DM, and $K_{1,2}$ are modified Bessel functions. This condition, in turn, puts a constraint on the DM-HNL coupling y_χ. For lighter M_1, the DM remains out of equilibrium for a longer period of time before it equilibrates, since in that case the decay width becomes comparatively smaller, making the decay lifetime longer. In order for the freeze-in production via decay to stay nonthermal till $T \simeq 1\,$GeV (the lowest reheating temperature we consider to avoid the BBN constraints), one needs a very small $y_\chi \lesssim 10^{-10}$.[1]

For DM production via scattering, we compare the rates of 2-to-2 scattering processes with the Hubble rate. The reaction rate for the scattering process is given by $\mathcal{R} = n_{\rm eq}\langle\sigma v\rangle \equiv \gamma_{\rm ann}/n_{\rm eq}$, where we consider $n_{\rm eq}$ to be the equilibrium number density of the SM particles in the initial state. In this case, the bound on y_χ can be significantly relaxed to $y_\chi \lesssim 10^{-7}$, as compared to the decay case mentioned above.

In the presence of DM production both via decay and scattering, the contribution from decay generally wins in the lower temperature region, where infrared freeze-in becomes important, i.e., where the DM yield becomes important at later times (low temperatures). Thus, in case the decay channel $N \to \chi\varphi$ is open, we can ignore the 2-to-2 DM production channels. Therefore, our analysis will be divided into two categories: (a) $M_1 > m_\chi + m_\varphi$ for which the DM production from decay is dominant, and (b) $M_1 \leq m_\chi + m_\varphi$ for which DM production from scattering is important (the decay is kinematically forbidden). In either case, we have four free parameters (assuming a fixed Higgs portal coupling $\lambda_{H\varphi}$): $\{M_1, m_\chi, m_\varphi, y_\chi\}$, which determine the viable parameter space for the DM.

3.2. DM Production via HNL Decay

For $M_1 > m_\chi + m_\varphi$, the DM production channel from HNL decay is kinematically available. The asymptotic DM yield can be analytically computed by integrating equation (17):

$$Y_\chi(T=0) \approx \frac{405 g_N}{4\pi^2 g_{\star s}\sqrt{g_{\star\rho}}}\sqrt{\frac{5}{2}}\frac{M_P \Gamma_{N_1\to\chi\varphi}}{M_1^2}, \tag{19}$$

where $g_N = 2$ is the number of degrees of freedom for HNL. Here, $g_{\star s}$ and $g_{\star\rho}$ are the effective numbers of relativistic degrees of freedom contributing to the entropy and energy density, respectively, while M_P is the reduced Planck mass. The relic abundance at present epoch $T = T_0$ can then be obtained using

$$\Omega_\chi h^2 = \left(2.75\times 10^8\right)\left(\frac{m_\chi}{\rm GeV}\right) Y_\chi(T_0), \tag{20}$$

which needs to satisfy the value as measured by Planck: $\Omega_{\rm DM}h^2 = 0.11933 \pm 0.00091$ [61]. We find that the right relic density can be obtained for $y_\chi \lesssim 10^{-10}$ which is typically within the ballpark where nonthermal DM production is viable. With the increase in M_1, it is possible to obtain the correct

[1] This value, although much smaller than the typical Dirac Yukawa couplings, does not contradict anything and is stable against radiative corrections.

relic density for larger m_χ for a fixed y_χ since $Y_\chi \propto 1/M_1$. Similarly, on decreasing the DM Yukawa coupling y_χ, for a fixed M_1, one expects to obtain the right abundance for a larger DM mass. For $y_\chi \gtrsim 10^{-10}$, the DM can thermalize in the early Universe as mentioned earlier and freeze-in is no longer viable. It is important to note here that for $M_1 \lesssim \mathcal{O}\,(\mathrm{MeV})$, the DM mass has to be extremely light for $y_\chi \sim 10^{-10}$ to satisfy the relic abundance. However, this is constrained by the measurements of the free-streaming of warm DM (WDM) from Lyman-α flux-power spectra [62, 63, 64, 65] which only allow a DM mass $\gtrsim$7.5 keV. For smaller y_χ, this constraint on the parameter space does not exist anymore since in that case one has to go to a heavier DM to satisfy the freeze-in relic density.

To obtain the net parameter space for the DM satisfying relic abundance, we scan over the DM and HNL masses, while keeping $m_\varphi = 2m_\chi$ and fixing the DM Yukawa coupling $y_\chi = 10^{-10}$, ensuring that the DM production via decay remains non-thermal as discussed earlier. We also fix $\mathrm{Re}[z] = 0.1$ and vary $\mathrm{Im}[z] \in [0.1, 7.0]$ in the CI parametrization (cf. equation (7)) for the Dirac Yukawa coupling. Note that $\mathrm{Im}[z] = 0$ would be the canonical seesaw case with very small active-sterile neutrino mixing, which is shown by the lower black dashed line in Figure 2, whereas the upper black dashed line corresponds to $\mathrm{Im}[z] = 7$ which is the rough upper limit on the mixing from charged lepton flavor violation [66]. Since the DM coupling y_χ that controls the relic abundance is uncorrelated with the HNL Yukawa coupling for the decay scenario (except for the tiny change in the HNL decay width), for a given choice of y_χ satisfying the relic density, it is always possible to have a viable parameter space in the HNL mass-mixing plane for the DM, which also satisfies the light neutrino mass constraints. This is shown by the green-shaded regions in Figure 2: the left panel for electron mixing (here U_{eN} stands for $(U_{\nu N})_{e1}$), the middle panel for muon mixing, and the right panel for tau mixing. The choice of y_χ is to ensure that the DM production takes place via freeze-in.

Also shown in Figure 2 are the current HNL exclusion regions (gray-shaded) from various cosmological observations (such as BBN, CMB, and Lyman-α), as well as laboratory constraints (such as beta decays, meson decays, beam-dump searches, precision electroweak tests, and direct collider searches); see [47, 67, 68, 69, 70, 71, 72] for details.[2] The future HNL sensitivities are also shown (unshaded curves) for comparison. We see that part of the DM relic density allowed parameter space for $\mathrm{Im}[z] \gtrsim 1$ lies within reach of future sensitivity of beam-dump and collider experiments. Because of $M_N^{-1/2}$ dependence (cf., equation (11)), a larger M_1 satisfies the light neutrino mass for comparatively lower $|U_{\nu N}|^2$, while the $|U_{\nu N}|^2$ coupling is boosted for higher $\mathrm{Im}[z]$, improving the experimental reach. A larger DM Yukawa requires a lighter DM to produce the observed abundance, which is constrained by the WDM limit due to Lyman-α constraints. Here, we have considered the conservative limit of 7.5 keV on fermion DM mass. This is shown by the black vertical line that forbids $M_1 \lesssim$ 1 MeV in the decay scenario. On considering a smaller DM Yukawa coupling, the parameter space remains unchanged, except that the WDM bound does not apply anymore since the DM mass is always found to be above the keV scale to satisfy the relic density bound. Our analysis presented here is for NH of neutrino masses.

3.3. *DM Production via HNL Scattering*

Next, let us take up the case where $M_1 < m_\chi + m_\varphi$, making only the 2-to-2 processes available for DM production. Because of both *s*- and *t*-channel contributions (cf. Figure 1), it is difficult to obtain an exact analytical solution of the BE in this case. However, it is easy to understand that the final DM yield and hence relic abundance has a $y_\chi^2 Y_D^2$ dependence on the couplings as the *t*-channel contribution is largely subdominant. We find that for larger m_χ a smaller y_χ is required for satisfying the relic bound as $\Omega_\chi h^2 \propto y_\chi^2 m_\chi$. Similarly, for a fixed DM mass, as we increase y_χ, we need to go to larger M_1 to satisfy the observed abundance, as that corresponds to smaller y_N (cf. equation (11)). The same is true for a fixed y_χ as we go to heavier DM mass since in that case overabundance can be avoided by choosing smaller y_N, i.e., heavier M_1. This feature is more prominent for larger y_χ. As we increase the DM mass, we need smaller y_χ to satisfy the relic bound. It is important to note here that in the case of scattering, we can always find a range of y_χ such that the DM is always safe from WDM limit unlike the case of decay. Small values of y_χ require heavier DM to satisfy the relic density constraint as $\Omega_\chi h^2 \propto m_\chi (y_\chi y_N)^2$. On the other hand, lowering y_χ moves the parameter space toward larger $|U_{\alpha N}|^2$ to compensate for underabundance accordingly. Similarly, for small $\mathrm{Im}[z]$, the allowed region shifts to smaller values of $|U_{\alpha N}|^2$.

We now cast the allowed DM relic density parameter space in the 2-to-2 scattering case onto the HNL parameter space in Figure 3. We project all the relevant limits in $|U_{\alpha N}|^2 - M_1$ as we did in case of decay (cf. Figure 2). Here, we find that the viable parameter space gradually diminishes toward the right, making a wedge-like shape. This is attributed to the fact that in order to have a dominant contribution from scattering, we confine ourselves only in the region of the parameter space where $M_1 < m_\chi$, which kinematically forbids the decay channel since we have chosen $m_\varphi = 2m_\chi$. Another important feature is the absence of the constraint on WDM due to Ly-α here. This is due to the freedom of choosing larger y_χ in this case, which can still reproduce the correct abundance with a smaller y_N, without lowering the DM mass. In the case of decay, this was not possible as the only coupling controlling the DM abundance was y_χ; hence, a larger y_χ resulted in a lighter DM, making the WDM bound more stringent.

We should also mention here the possibility that the Yukawa couplings of HNLs can carry new sources of CP violation, and their out-of-equilibrium decays can produce a lepton asymmetry, which can then be transferred to a baryon asymmetry by the electroweak sphalerons—this is the standard leptogenesis mechanism [73]. Although the vanilla leptogenesis requires HNL mass to be way above the electroweak scale ($\gtrsim 10^9$ GeV) [74], low-scale leptogenesis with HNLs accessible to laboratory experiments is also feasible, either via resonant leptogenesis [75, 76] or via HNL oscillations [77, 78] or both [79]. Therefore, in the present scenario, it is possible to have a simultaneous explanation of DM relic density and baryon asymmetry since both rely on the interactions of the HNLs. For instance, as has already been discussed in [79, 80], it is possible to have successful leptogenesis considering two nearly degenerate HNLs in the GeV range, with

[2] The data used for plotting the constraints is available on the website `www.sterile-neutrino.org`.

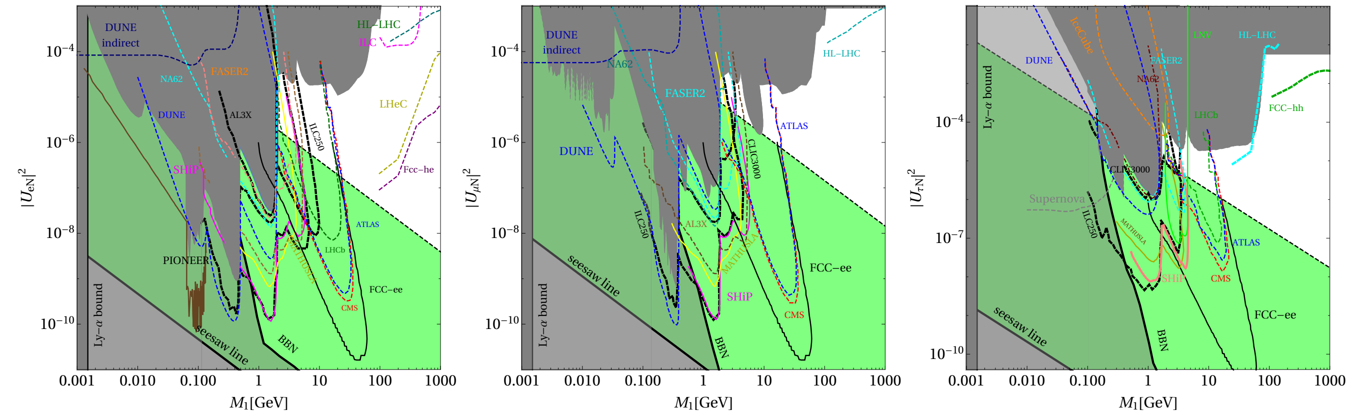

FIGURE 2: Freeze-in DM region in the HNL decay scenario superimposed in the plane of HNL mass and its coupling to the electron, muon, and tau flavors. In each panel, the green-shaded region corresponds to the observed DM abundance in the HNL parameter space for a normal hierarchy of neutrino masses. The gray-shaded regions are excluded by various HNL constraints. The future HNL sensitivities are also shown for comparison. See text and [40] for details.

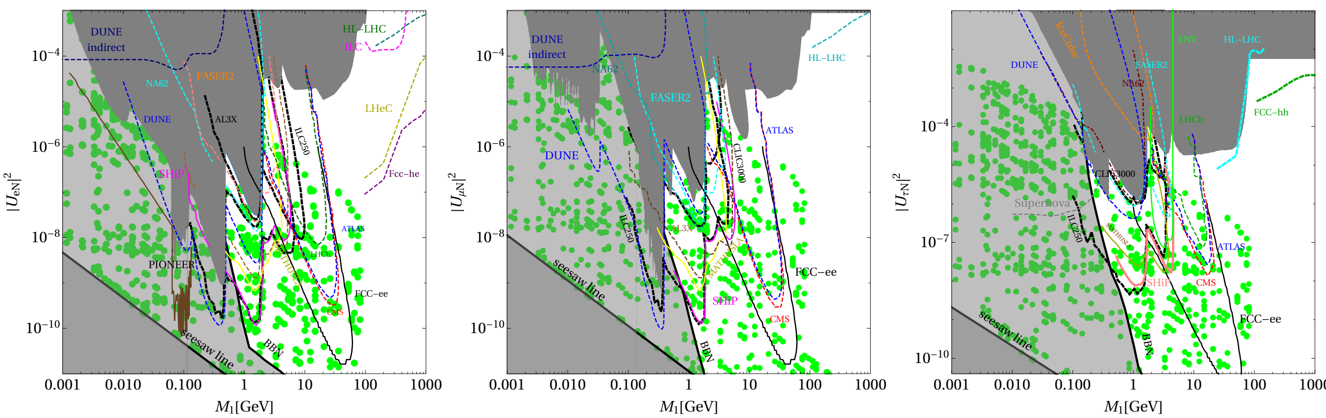

FIGURE 3: Similar to Figure 2 but for the 2-to-2 scattering case.

$|U|^2 = \sum_\alpha |U_\alpha N|^2 \sim \mathcal{O}(10^{-10}\text{–}10^{-8})$, which is also consistent with the DM relic density as shown in Figures 2 and 3.

4. THE FATE OF φ

For completeness, let us discuss what happens to the new scalar singlet φ in this model. First of all, note that φ is non-thermally produced along with the DM χ unavoidably from N_1 decay or 2-to-2 scattering mediated by N_1 (cf. Figure 1).[3] On the other hand, φ can also be produced from the 2-to-2 scattering of the bath particles due to the presence of the portal interaction $|H|^2\varphi^2$ (cf. equation (15)). This leads to φ production via contact interaction before electroweak symmetry breaking and also via s-channel Higgs mediation once the electroweak symmetry is broken, and all the SM states become massive. For the range of masses we are interested in, φ can be as light as $\mathcal{O}$(MeV) and can be produced via on-shell decay of the Higgs after electroweak symmetry breaking. In that scenario, a large portal coupling $\lambda_{H\varphi}$ will then contribute to the Higgs invisible branching ratio $\mathrm{BR}(h \to \varphi\varphi)$, and from the most stringent LHC constraint on $\mathrm{BR}(h \to \text{invisible}) < 0.145$ [81] (see also [82] for a slightly weaker bound of 0.18), we find an upper bound of $\lambda_{H\varphi} \lesssim 6 \times 10^{-3}$ for $m_\varphi < m_h/2$.

After the φ's are produced in the early Universe, the next question is their stability. For $m_\varphi < M_N$, the only possible decay mode of φ is a 3-body final state with DM and SM via off-shell HNL. For $m_\varphi \gtrsim 100\,\text{GeV}$, we consider the 3-body decays of $\varphi \to \chi N^* \to \chi\nu h, \chi\nu Z, \chi\ell^\pm W^\mp$. The dependence of the decay width on the free parameters can be approximately obtained via dimensional analysis as

$$\Gamma_\varphi^{\text{3-body}} \sim (y_\chi Y_D)^2 \frac{m_\varphi^5}{M_1^4}, \tag{21}$$

where Y_D is determined by equation (7). Thus, the decay width (lifetime) increases (decreases) with m_φ, while it has an inverse dependence on the HNL mediator mass. We numerically calculate the total 3-body decay width of φ (taking all possible final states into account) and obtain the corresponding lifetime $\tau_\varphi \equiv \Gamma_\varphi^{-1}$ as a function of m_φ. We find that for certain choices of mass and coupling, φ can have a lifetime larger than the age of

[3] There can be 2-to-2 scattering via t-channel χ as well, but that contribution is sub-dominant because of negligible initial abundance of χ and y_χ^4 dependence of the cross section.

the Universe $\tau_U \simeq 4.35 \times 10^{17}$ sec; however, it is still way below the typical bound on DM lifetime $\gtrsim 10^{26}$ sec [83] and φ cannot be a DM candidate in our model.

As mentioned before, the scalar φ can be produced from the bath because of the presence of the portal interaction, controlled by the coupling $\lambda_{H\varphi}$, on top of its production from the on-shell decay of HNL or HNL mediated 2-to-2 process. The production of φ involving HNL is already out of equilibrium for the coupling choice of our interest that leads to freeze-in production of the DM. For the processes involving the Higgs portal coupling $\lambda_{H\varphi}$, we find that with $\lambda_{H\varphi} \lesssim 10^{-5}$, the φ production rate stays out of equilibrium till $T \simeq 1\,\mathrm{GeV}$, irrespective of m_φ. Therefore, the φ particles do not contribute to N_{eff} and we are safe from the cosmology bounds on ΔN_{eff}.

It is, however, important to note that for $m_\varphi < 100\,\mathrm{GeV}$, where only 4-body decays are allowed, the scalar lifetime can be significantly larger because of its tiny decay width. For instance, we numerically estimated that $\Gamma_{\varphi \to \chi \nu b \bar{b}} \sim 10^{-60}\,\mathrm{GeV}$ for $m_\varphi = 10\,\mathrm{GeV}$, $m_\chi = 0.1\,\mathrm{GeV}$, and $M_1 = 500\,\mathrm{GeV}$ with $y_\chi = 10^{-10}$ and $\mathrm{Im}[z] = 1$. This leads to a lifetime $\tau_\varphi \sim 10^{30}$ s. Therefore, for lighter m_φ, φ can also contribute to the DM abundance as it becomes stable over the cosmological scale. It is, however, possible to tune the portal coupling $\lambda_{H\varphi}$ such that the contribution of φ to the total relic abundance is negligibly small and χ is the dominant DM component.

5. OTHER POSSIBLE SIGNATURES

The standard collider signatures of the HNLs [84, 85, 86, 48], such as the dilepton (or trilepton) plus missing transverse energy, either prompt or displaced depending on the Dirac Yukawa couplings, are also applicable in our scenario. Moreover, the presence of the singlet scalar φ, in addition to the HNLs, opens up the possibility of distinguishing this model at colliders from the pure seesaw models, since φ contributes to missing transverse energy at colliders. For $M_1 > m_\varphi + m_\chi$, the branching ratios (BRs) of the HNLs into the SM final states, i.e., $N \to \ell W, \nu Z, \nu h$, get modified due to the presence of the additional decay mode $N \to \chi\varphi$, depending on the new Yukawa coupling y_χ. Note that the same Yukawa coupling y_χ governs the DM production in our freeze-in scenario; therefore, measuring the BRs accurately can in principle give us a direct collider probe of the HNL coupling to the DM. However, it turns out to be extremely difficult in practice. The reason is that for the decay case, the coupling y_χ is required to be very small, $\lesssim 10^{-10}$ (cf. Section 3.2). For comparison, the HNL couplings to the SM fermions, governed by the Dirac Yukawa couplings, are typical of the order of 10^{-6} for the canonical seesaw case (for a 100 GeV-scale HNL) and can be much larger for larger $\mathrm{Im}[z]$. Therefore, the HNL decay into the SM final states, either two-body (for $M_N > m_W$) or three-body (for $M_N < m_W$), is always expected to be dominant over the new channel $N \to \chi\varphi$. We have numerically checked that for the parameter space we are interested in here, $\mathrm{BR}(N \to \chi\varphi)$ can be at most of the order of 10^{-5} for lighter HNLs, and much smaller for heavier HNLs. Therefore, we do not expect any observable excess in the HNL invisible decay mode (due to $N \to \chi\varphi$) over the standard one ($N \to 3\nu$).

It is also possible to directly produce φ at hadron colliders via gluon fusion, $gg \to h \to \varphi\varphi$, using the trilinear coupling $\lambda_{H\varphi}$. This is very similar to a generic SM-singlet scalar search at the LHC; see, e.g., [87]. However, the production cross-section will be heavily suppressed not only because of the loop-induced Higgs production channel but also due to the requirement that $\lambda_{H\varphi} \lesssim 10^{-5}$ in order to prevent φ from coming into thermal equilibrium with the SM plasma (cf. Section 4). Therefore, the collider prospects of φ, for instance, in the monojet channel, are not so promising in our case. Before concluding, we note that the freeze-in scenario considered here can in principle also lead to some DM direct detection as well as indirect detection signatures. As for direct detection, it will be induced by a loop-induced effective DM coupling to the Z-boson [22, 52]. However, for the y_χ values considered here, the corresponding direct detection cross sections turn out to be many orders of magnitude below the current constraints [88]. As for indirect detection, promising prospects were discussed in [19] for the freeze-out scenario; this, however, is not the case for our freeze-in scenario where the DM annihilation process is not that efficient, simply because of the huge suppression of the DM number density by the factor of $n_\chi / n_\chi^{\mathrm{eq}}$ as compared to the freeze-out case. On the other hand, the neutrino flux from φ decay might be accessible in high-energy neutrino experiments [33].

6. CONCLUSION

We have looked into the possibility of probing freeze-in DM coupling via the heavy neutrino portal. We have minimally extended the type-I seesaw scenario with the addition of a gauge-singlet fermion χ and a real singlet scalar φ. Both φ and χ are considered to be odd under some stabilizing Z_2 symmetry and the fermion χ is considered to be the viable DM candidate given $m_\chi < m_\varphi$. The DM only talks to the SM sector via its coupling to the HNLs of the form $y_\chi N \chi \varphi$. Depending on whether M_N is lighter or heavier than the sum of m_χ and m_φ, the DM can be produced nonthermally either from the decay of the HNLs, considered to be part of the thermal bath, or via 2-to-2 scattering of the SM particles mediated by the HNLs. This is referred to here as the heavy neutrino portal freeze-in. Using the Casas-Ibarra parametrization to satisfy the neutrino oscillation data with two HNLs, we are left with four free parameters of the model: the DM mass m_χ, DM Yukawa coupling with the HNL y_χ, the mass of the new singlet scalar m_φ, and the lightest HNL mass M_1.

We find that the requirement for freeze-in production of DM (together with the Planck-observed relic abundance) necessarily requires the DM Yukawa coupling $y_\chi \lesssim 10^{-10}$ in case the DM is produced from the on-shell decay of the HNL, while for scattering this bound can be significantly relaxed to $y_\chi \lesssim 10^{-7}$ because of the involvement of HNL Yukawa couplings with the SM. Assuming sizable active-sterile neutrino mixing with HNL mass lying in the MeV-TeV range, our HNL portal scenario can fall within the reach of several current and future facilities, including collider, beam-dump, and forward physics experiments, which typically look for feebly coupled HNLs, as shown in Figures 2 and 3. This, in turn, provides a complementary window to probe the freeze-in DM parameter space.

CONFLICTS OF INTEREST

The author declares that there are no conflicts of interest regarding the publication of this paper.

ACKNOWLEDGMENTS

The work of BD was supported in part by the U.S. Department of Energy under Grant No. DE-SC0017987.

References

[1] Gianfranco Bertone and Tim M. P. Tait. A new era in the search for dark matter. *Nature*, 562(7725):51–56, 2018.
[2] Gary Steigman and Michael S. Turner. Cosmological Constraints on the Properties of Weakly Interacting Massive Particles. *Nucl. Phys. B*, 253:375–386, 1985.
[3] Gary Steigman, Basudeb Dasgupta, and John F. Beacom. Precise Relic WIMP Abundance and its Impact on Searches for Dark Matter Annihilation. *Phys. Rev.*, D86:023506, 2012.
[4] Giorgio Arcadi, Maíra Dutra, Pradipta Ghosh, Manfred Lindner, Yann Mambrini, Mathias Pierre, Stefano Profumo, and Farinaldo S. Queiroz. The waning of the WIMP? A review of models, searches, and constraints. *Eur. Phys. J. C*, 78(3):203, 2018.
[5] Leszek Roszkowski, Enrico Maria Sessolo, and Sebastian Trojanowski. WIMP dark matter candidates and searches—current status and future prospects. *Rept. Prog. Phys.*, 81(6):066201, 2018.
[6] Jodi Cooley et al. Report of the Topical Group on Particle Dark Matter for Snowmass 2021. 9 2022.
[7] Vanda Silveira and A. Zee. Scalar Phantoms. *Phys. Lett. B*, 161:136–140, 1985.
[8] John McDonald. Gauge singlet scalars as cold dark matter. *Phys. Rev.*, D50:3637–3649, 1994.
[9] Peter Galison and Aneesh Manohar. Two Z's or not two Z's? *Phys. Lett. B*, 136:279–283, 1984.
[10] Bob Holdom. Two $U(1)$'s and Epsilon Charge Shifts. *Phys. Lett. B*, 166:196–198, 1986.
[11] Maxim Pospelov, Adam Ritz, and Mikhail B. Voloshin. Secluded WIMP Dark Matter. *Phys. Lett. B*, 662:53–61, 2008.
[12] Adam Falkowski, Jose Juknevich, and Jessie Shelton. Dark Matter Through the Neutrino Portal. 8 2009.
[13] John F. Cherry, Alexander Friedland, and Ian M. Shoemaker. Neutrino Portal Dark Matter: From Dwarf Galaxies to IceCube. 11 2014.
[14] Vannia Gonzalez Macias and Jose Wudka. Effective theories for Dark Matter interactions and the neutrino portal paradigm. *JHEP*, 07:161, 2015.
[15] Vannia González-Macías, José I. Illana, and José Wudka. A realistic model for Dark Matter interactions in the neutrino portal paradigm. *JHEP*, 05:171, 2016.
[16] Miguel Escudero, Nuria Rius, and Verónica Sanz. Sterile neutrino portal to Dark Matter I: The $U(1)_{B-L}$ case. *JHEP*, 02:045, 2017.
[17] Miguel Escudero, Nuria Rius, and Verónica Sanz. Sterile Neutrino portal to Dark Matter II: Exact Dark symmetry. *Eur. Phys. J. C*, 77(6):397, 2017.
[18] Yi-Lei Tang and Shou-hua Zhu. Dark Matter Relic Abundance and Light Sterile Neutrinos. *JHEP*, 01:025, 2017.
[19] Brian Batell, Tao Han, and Barmak Shams Es Haghi. Indirect Detection of Neutrino Portal Dark Matter. *Phys. Rev. D*, 97(9):095020, 2018.
[20] Brian Batell, Tao Han, David McKeen, and Barmak Shams Es Haghi. Thermal Dark Matter Through the Dirac Neutrino Portal. *Phys. Rev. D*, 97(7):075016, 2018.
[21] Miguel G. Folgado, Germán A. Gómez-Vargas, Nuria Rius, and Roberto Ruiz De Austri. Probing the sterile neutrino portal to Dark Matter with γ rays. *JCAP*, 08:002, 2018.
[22] Mathias Becker. Dark Matter from Freeze-In via the Neutrino Portal. *Eur. Phys. J. C*, 79(7):611, 2019.
[23] Marco Chianese and Stephen F. King. The Dark Side of the Littlest Seesaw: freeze-in, the two right-handed neutrino portal and leptogenesis-friendly fimpzillas. *JCAP*, 09:027, 2018.
[24] Asher Berlin and Nikita Blinov. Thermal neutrino portal to sub-MeV dark matter. *Phys. Rev. D*, 99(9):095030, 2019.
[25] Priyotosh Bandyopadhyay, Eung Jin Chun, Rusa Mandal, and Farinaldo S. Queiroz. Scrutinizing Right-Handed Neutrino Portal Dark Matter With Yukawa Effect. *Phys. Lett. B*, 788:530–534, 2019.
[26] Ligong Bian and Yi-Lei Tang. Thermally modified sterile neutrino portal dark matter and gravitational waves from phase transition: The Freeze-in case. *JHEP*, 12:006, 2018.
[27] Marco Chianese, Bowen Fu, and Stephen F. King. Minimal Seesaw extension for Neutrino Mass and Mixing, Leptogenesis and Dark Matter: FIMPzillas through the Right-Handed Neutrino Portal. *JCAP*, 03:030, 2020.
[28] Marco Chianese, Bowen Fu, and Stephen F. King. Interplay between neutrino and gravity portals for FIMP dark matter. *JCAP*, 01:034, 2021.
[29] J. M. Lamprea, E. Peinado, S. Smolenski, and J. Wudka. Self-interacting neutrino portal dark matter. *Phys. Rev. D*, 103(1):015017, 2021.
[30] M. Blennow, E. Fernandez-Martinez, A. Olivares-Del Campo, S. Pascoli, S. Rosauro-Alcaraz, and A. V. Titov. Neutrino Portals to Dark Matter. *Eur. Phys. J. C*, 79(7):555, 2019.
[31] Hiren H. Patel, Stefano Profumo, and Bibhushan Shakya. Loop dominated signals from neutrino portal dark matter. *Phys. Rev. D*, 101(9):095001, 2020.
[32] Catarina Cosme, Maíra Dutra, Teng Ma, Yongcheng Wu, and Litao Yang. Neutrino portal to FIMP dark matter with an early matter era. *JHEP*, 03:026, 2021.
[33] Priyotosh Bandyopadhyay, Eung Jin Chun, and Rusa Mandal. Feeble neutrino portal dark matter at neutrino detectors. *JCAP*, 08:019, 2020.
[34] Anirban Biswas, Debasish Borah, and Dibyendu Nanda. Light Dirac neutrino portal dark matter with observable $\Delta N_{\rm eff}$. *JCAP*, 10:002, 2021.
[35] Arghyajit Datta, Rishav Roshan, and Arunansu Sil. Imprint of the Seesaw Mechanism on Feebly Interacting Dark Matter and the Baryon Asymmetry. *Phys. Rev. Lett.*, 127(23):231801, 2021.
[36] Yu Cheng, Wei Liao, and Qi-Shu Yan. Collider search of light dark matter model with dark sector decay. *Chin. Phys. C*, 46(6):063103, 2022.
[37] Debasish Borah, Manoranjan Dutta, Satyabrata Mahapatra, and Narendra Sahu. Self-interacting dark matter via right handed neutrino portal. *Phys. Rev. D*, 105(1):015004, 2022.
[38] Anirban Biswas, Debasish Borah, Nayan Das, and Dibyendu Nanda. Freeze-in Dark Matter and $\Delta N_{\rm eff}$ via Light Dirac Neutrino Portal. 5 2022.
[39] Ang Liu, Feng-Lan Shao, Zhi-Long Han, Yi Jin, and Honglei Li. Sterile Neutrino Portal Dark Matter in νTHDM. 5 2022.

[40] Basabendu Barman, P. S. Bhupal Dev, and Anish Ghoshal. Probing Freeze-in Dark Matter via Heavy Neutrino Portal. 10 2022.

[41] Peter Minkowski. $\mu \to e\gamma$ at a Rate of One Out of 10^9 Muon Decays? *Phys. Lett. B*, 67:421–428, 1977.

[42] Rabindra N. Mohapatra and Goran Senjanovic. Neutrino Mass and Spontaneous Parity Nonconservation. *Phys. Rev. Lett.*, 44:912, 1980.

[43] Murray Gell-Mann, Pierre Ramond, and Richard Slansky. Complex Spinors and Unified Theories. *Conf. Proc. C*, 790927:315–321, 1979.

[44] Tsutomu Yanagida. Horizontal gauge symmetry and masses of neutrinos. *Conf. Proc. C*, 7902131:95–99, 1979.

[45] S. L. Glashow. The Future of Elementary Particle Physics. *NATO Sci. Ser. B*, 61:687, 1980.

[46] J. Schechter and J. W. F. Valle. Neutrino Masses in $SU(2) \times U(1)$ Theories. *Phys. Rev. D*, 22:2227, 1980.

[47] Patrick D. Bolton, Frank F. Deppisch, and P. S. Bhupal Dev. Neutrinoless double beta decay versus other probes of heavy sterile neutrinos. *JHEP*, 03:170, 2020.

[48] Asli M. Abdullahi et al. The Present and Future Status of Heavy Neutral Leptons. In *2022 Snowmass Summer Study*, 3 2022.

[49] Lawrence J. Hall, Karsten Jedamzik, John March-Russell, and Stephen M. West. Freeze-In Production of FIMP Dark Matter. *JHEP*, 03:080, 2010.

[50] Nicolás Bernal, Matti Heikinheimo, Tommi Tenkanen, Kimmo Tuominen, and Ville Vaskonen. The Dawn of FIMP Dark Matter: A Review of Models and Constraints. *Int. J. Mod. Phys. A*, 32(27):1730023, 2017.

[51] G. Bélanger et al. LHC-friendly minimal freeze-in models. *JHEP*, 02:186, 2019.

[52] Thomas Hambye, Michel H. G. Tytgat, Jérôme Vandecasteele, and Laurent Vanderheyden. Dark matter direct detection is testing freeze-in. *Phys. Rev. D*, 98(7):075017, 2018.

[53] Luc Darmé, Andrzej Hryczuk, Dimitrios Karamitros, and Leszek Roszkowski. Forbidden frozen-in dark matter. *JHEP*, 11:159, 2019.

[54] Basabendu Barman and Anish Ghoshal. Scale invariant FIMP miracle. *JCAP*, 03(03):003, 2022.

[55] Basabendu Barman and Anish Ghoshal. Probing pre-BBN era with Scale Invarint FIMP. 3 2022.

[56] J. A. Casas and A. Ibarra. Oscillating neutrinos and $\mu \to e, \gamma$. *Nucl. Phys. B*, 618:171–204, 2001.

[57] P. H. Frampton, S. L. Glashow, and T. Yanagida. Cosmological sign of neutrino CP violation. *Phys. Lett. B*, 548:119–121, 2002.

[58] Xiao-Gang He, Sechul Oh, Jusak Tandean, and Chung-Cheng Wen. Large Mixing of Light and Heavy Neutrinos in Seesaw Models and the LHC. *Phys. Rev. D*, 80:073012, 2009.

[59] P. Hernandez, M. Kekic, and J. Lopez-Pavon. Low-scale seesaw models versus $N_{\rm eff}$. *Phys. Rev. D*, 89(7):073009, 2014.

[60] P. Hernandez, M. Kekic, and J. Lopez-Pavon. $N_{\rm eff}$ in low-scale seesaw models versus the lightest neutrino mass. *Phys. Rev. D*, 90(6):065033, 2014.

[61] N. Aghanim et al. Planck 2018 results. VI. Cosmological parameters. *Astron. Astrophys.*, 641:A6, 2020.

[62] Julien Baur, Nathalie Palanque-Delabrouille, Christophe Yèche, Christophe Magneville, and Matteo Viel. Lyman-alpha Forests cool Warm Dark Matter. *JCAP*, 08:012, 2016.

[63] Vid Iršič et al. New Constraints on the free-streaming of warm dark matter from intermediate and small scale Lyman-α forest data. *Phys. Rev. D*, 96(2):023522, 2017.

[64] Guillermo Ballesteros, Marcos A. G. Garcia, and Mathias Pierre. How warm are non-thermal relics? Lyman-α bounds on out-of-equilibrium dark matter. *JCAP*, 03:101, 2021.

[65] Francesco D'Eramo and Alessandro Lenoci. Lower mass bounds on FIMP dark matter produced via freeze-in. *JCAP*, 10:045, 2021.

[66] P. S. Bhupal Dev, Srubabati Goswami, and Manimala Mitra. TeV Scale Left-Right Symmetry and Large Mixing Effects in Neutrinoless Double Beta Decay. *Phys. Rev. D*, 91(11):113004, 2015.

[67] Alexey Boyarsky, Maksym Ovchynnikov, Oleg Ruchayskiy, and Vsevolod Syvolap. Improved big bang nucleosynthesis constraints on heavy neutral leptons. *Phys. Rev. D*, 104(2):023517, 2021.

[68] Kyrylo Bondarenko, Alexey Boyarsky, Juraj Klaric, Oleksii Mikulenko, Oleg Ruchayskiy, Vsevolod Syvolap, and Inar Timiryasov. An allowed window for heavy neutral leptons below the kaon mass. *JHEP*, 07:193, 2021.

[69] Iryna Boiarska, Alexey Boyarsky, Oleksii Mikulenko, and Maksym Ovchynnikov. Constraints from the CHARM experiment on heavy neutral leptons with tau mixing. *Phys. Rev. D*, 104(9):095019, 2021.

[70] Patrick D. Bolton, Frank F. Deppisch, and P. S. Bhupal Dev. Probes of Heavy Sterile Neutrinos. In *56th Rencontres de Moriond on Electroweak Interactions and Unified Theories*, 6 2022.

[71] Ryan Barouki, Giacomo Marocco, and Subir Sarkar. Blast from the past II: Constraints on heavy neutral leptons from the BEBC WA66 beam dump experiment. 7 2022.

[72] Mihoko M. Nojiri, Yasuihito Sakaki, Kohsaku Tobioka, and Daiki Ueda. First Evaluation of Meson and τ lepton Spectra and Search for Heavy Neutral Leptons at ILC Beam Dump. 6 2022.

[73] M. Fukugita and T. Yanagida. Baryogenesis Without Grand Unification. *Phys. Lett.*, B174:45–47, 1986.

[74] Sacha Davidson and Alejandro Ibarra. A Lower bound on the right-handed neutrino mass from leptogenesis. *Phys. Lett. B*, 535:25–32, 2002.

[75] Apostolos Pilaftsis and Thomas E. J. Underwood. Resonant leptogenesis. *Nucl. Phys.*, B692:303–345, 2004.

[76] P. S. Bhupal Dev, Mathias Garny, Juraj Klaric, Peter Millington, and Daniele Teresi. Resonant enhancement in leptogenesis. *Int. J. Mod. Phys.*, A33:1842003, 2018.

[77] Evgeny K. Akhmedov, V. A. Rubakov, and A. Yu. Smirnov. Baryogenesis via neutrino oscillations. *Phys. Rev. Lett.*, 81:1359–1362, 1998.

[78] M. Drewes, B. Garbrecht, P. Hernandez, M. Kekic, J. Lopez-Pavon, J. Racker, N. Rius, J. Salvado, and D. Teresi. ARS Leptogenesis. *Int. J. Mod. Phys. A*, 33(05n06):1842002, 2018.

[79] Juraj Klarić, Mikhail Shaposhnikov, and Inar Timiryasov. Uniting Low-Scale Leptogenesis Mechanisms. *Phys. Rev. Lett.*, 127(11):111802, 2021.

[80] Pilar Hernandez, Jacobo Lopez-Pavon, Nuria Rius, and Stefan Sandner. Bounds on right-handed neutrino parameters from observable leptogenesis. 7 2022.

[81] Georges Aad et al. Search for invisible Higgs-boson decays in events with vector-boson fusion signatures using

139 fb^{-1} of proton-proton data recorded by the ATLAS experiment. 2 2022.

[82] Armen Tumasyan et al. Search for invisible decays of the Higgs boson produced via vector boson fusion in proton-proton collisions at $\sqrt{s} = 13$ TeV. *Phys. Rev. D*, 105:092007, 2022.

[83] Yann Mambrini, Stefano Profumo, and Farinaldo S. Queiroz. Dark Matter and Global Symmetries. *Phys. Lett. B*, 760:807–815, 2016.

[84] Anupama Atre, Tao Han, Silvia Pascoli, and Bin Zhang. The Search for Heavy Majorana Neutrinos. *JHEP*, 05:030, 2009.

[85] Frank F. Deppisch, P. S. Bhupal Dev, and Apostolos Pilaftsis. Neutrinos and Collider Physics. *New J. Phys.*, 17(7):075019, 2015.

[86] Yi Cai, Tao Han, Tong Li, and Richard Ruiz. Lepton Number Violation: Seesaw Models and Their Collider Tests. *Front. in Phys.*, 6:40, 2018.

[87] Elina Fuchs, Oleksii Matsedonskyi, Inbar Savoray, and Matthias Schlaffer. Collider searches for scalar singlets across lifetimes. *JHEP*, 04:019, 2021.

[88] J. Aalbers et al. First Dark Matter Search Results from the LUX-ZEPLIN (LZ) Experiment. 7 2022.